Int. J. Heat Mass Transfer. Vol. 36, No. 7, pp. 1875–1881, 1993
Printed in Great Britain

0017–9310/93 $6.00 + 0.00
Pergamon Press Ltd

# Thermocapillary breakdown of falling liquid films at high Reynolds numbers

MARK S. BOHN
National Renewable Energy Laboratory, 1617 Cole Blvd, Golden, CO 80401, U.S.A.

and

STEPHEN H. DAVIS
Department of Engineering Sciences and Applied Mathematics, Northwestern University, Evanston, IL 60208, U.S.A.

(*Received* 30 *April* 1992 *and in final form* 4 *August* 1992)

**Abstract**—This paper presents a new correlation in which the heat flux required to break a falling liquid film can be determined from the film Reynolds number. The correlation is based on the balance of local forces in the substrate region for high-Reynolds number films. Validation of the correlation required experimental data for breakdown of wavy liquid films at a significantly higher Reynolds number and heat flux than have been presented in the past. These data are also presented in the paper. The results show that the correlation collapses the experimental data for three liquids with widely varying physical properties at film Reynolds numbers at up to about $10^4$. This correlation gives one the ability to predict the thermocapillary breakdown of wavy falling films at high Reynolds number, high heat flux, and over a wide range of fluid properties.

## 1. INTRODUCTION

FLOWING liquid films are used in a large number of heat- and mass-transfer applications including falling-film evaporators, film cooling of rocket nozzles and turbine blades, nuclear-reactor cooling, packed columns, vertical condensers, and wetted-wall columns. High transfer coefficients are the main incentive for using thin liquid films. However, the free surface of the film is susceptible to disruption by a number of phenomena such as gas-flow shear, evaporation, boiling, and thermocapillary effects. Through the loss of transfer area, any of these mechanisms can, at best, reduce overall transfer rates and at worst lead to equipment damage.

In this paper, we are concerned with the disruption of falling liquid films by thermocapillary effects. For most liquids, surface tension decreases with increasing temperature. If a localized area of the film is warmer than surrounding areas, because of nonuniform heating, for example, the resulting surface tension forces will tend to pull fluid away from the area. The thinner film is less capable of removing heat, so its temperature rises further. Surface tension forces then increase more and the film thins more, until finally the film breaks, leaving a dry spot on the surface. If heat flux is being controlled, the surface temperature may rise until the surface is damaged. Even if the surface is not damaged, the reduced surface area available for heat transfer reduces the overall heat transfer effectiveness of the system.

The present work was motivated by the application of falling liquid films to solar energy utilization. In the central receiver concept, a field of mirrors (heliostats) tracks the sun so that its image is fixed on a central target, or receiver. A cooling fluid circulates in the receiver and delivers the energy to a heat engine. Typically, the receiver would be configured as a multitude of tubes through which the cooling fluid circulates. In a relatively new concept called the Direct Absorption Receiver, the cooling fluid is allowed to flow under the influence of gravity down an inclined metal surface. Although this concept promises significantly lower costs because of design simplicity, a number of technical issues regarding the operation of the falling film arise [1]. One such issue is the susceptibility of the film to breakdown under the influence of the relatively high solar flux that is present at the receiver surface. Since the heliostats do not produce a uniform flux, film breakdown can result. In addition, because the film operates at high Reynolds numbers, free-surface instabilities are present and so it is wavy. This means that some areas on the film are thinner than others, and film breakdown can begin at these areas.

In attempting to assess the feasibility of the concept, Newell *et al.* [1] noted that methods for predicting the breakdown of falling liquid films were lacking. In this paper, we present experimental data and a relatively simple model of the breakdown phenomenon that leads to a correlation giving predictions of the heat flux required to break a falling liquid film.

## NOMENCLATURE

| | | | |
|---|---|---|---|
| $c_p$ | specific heat [J kg$^{-1}$ K$^{-1}$] | $U_{TC}$ | thermocapillary speed [m s$^{-1}$] |
| $g$ | acceleration of gravity [m s$^{-2}$] | $u$ | film-flow velocity in the $x$ direction [m s$^{-1}$] |
| $h_0$ | mean substrate thickness [m] | $v$ | film-flow velocity in the $y$ direction [m s$^{-1}$] |
| $l_x$ | downstream length scale [m] | $w$ | film-flow velocity in the $z$ direction [m s$^{-1}$] |
| $l_y$ | lateral length scale [m] | $x$ | downstream coordinate [m] |
| $m$ | correlation constant [—] | $y$ | cross-stream coordinate [m] |
| $q_W$ | breakdown flux [W m$^{-2}$] | $z$ | plate-normal coordinate [m]. |
| $q_W^{(s)}$ | scale for breakdown flux [W m$^{-2}$] | | |
| $n$ | correlation constant [—] | Greek symbols | |
| $Re$ | overall film Reynolds number, $[4\Gamma/\mu]$ | $\Gamma$ | liquid mass-flow rate per unit width [kg m$^{-1}$ s$^{-1}$] |
| $Re_s$ | substrate Reynolds number | $\mu$ | viscosity [kg m$^{-1}$ s$^{-1}$] |
| $T$ | temperature [K] | $\nu$ | kinematic viscosity [m$^2$ s$^{-1}$] |
| $u$ | film flow velocity in the downward direction [m s$^{-1}$] | $\rho$ | density [kg m$^{-3}$] |
| $U_H$ | hydrodynamic speed [m s$^{-1}$] | $\sigma$ | surface tension [N m$^{-1}$]. |

## 2. BACKGROUND

Falling-film breakdown is usually exhibited by the formation of dry spots in the flow. These dry spots extend downstream, giving a pattern of rivulets in which the full upstream flow is conveyed into thin fingers of liquid. The conditions for the creation of this longitudinal configuration have been the object of many investigations.

Chung and Bankoff [2] proposed a minimum energy condition as the criterion for rivulet formation. Here, the total energies of two states are compared, an array of rivulets and the continuous film; the state with the lower total energy is preferred.

It is only recently that rivulets have been shown to develop under dynamic conditions. Joo *et al.* [3] have derived an evolution equation that gives the development in space and time of the interface of a heated falling-film. This film is susceptible to surface-wave and thermocapillary instabilities, neither of which will separately lead to rivulets. However, by numerical integration of the evolution equation, Joo *et al.* find that nonlinear interaction of the instabilities does lead to the development of longitudinal structures. The limitations of this analysis are that the Reynolds numbers and heat fluxes have to be rather small while the emphasis of the present work is high Reynolds numbers and high heat fluxes.

At Reynolds numbers above about 25, free-surface instabilities result in the development of roll waves on the film surface. Between these roll waves there exists a thin liquid film known as the substrate. These features are described in detail by Chu and Dukler [4]. At a fixed location the surface supporting the film flow is alternately covered by roll waves and the substrate. Because of these complexities when the Reynolds numbers are substantial, one must employ empirical methods to make progress with respect to thermocapillary breakdown.

The idea that thermocapillarity is an important ingredient for the breakdown of nonisothermal, nonvolatile films goes back to Norman and McIntyre [5]. Simon and Hsu [6] used this idea in developing a correlation. They used lubrication arguments (inconsistently) and obtained a criterion for dryout that depends on a critical thickness. A difficulty with this approach is that this critical thickness is not given by theory; it must be known ahead of time. Fujita and Ueda [7] use a variant of this idea to obtain a breakdown criterion for nonuniform films.

The aim of the present work is to examine theoretically and experimentally the breakdown of films on vertical surfaces that have sizeable Reynolds numbers and heat fluxes. The correlation is based on simple force balances, involving thermocapillarity, and is free of critical-thickness estimates. The experiment obtains data at higher values of Reynolds numbers and heat fluxes than have been obtained before and utilizes the derived correlation for data analysis.

## 3. CORRELATION OF BREAKDOWN FLUX VS REYNOLDS NUMBER

The object here is the formulation of a relation that correlates the appearance of dryout with flow parameters without the presence of *ad hoc* estimates of critical film thicknesses. We are concerned mainly with the film flow in the substrate since this is likely to be the part of the film flow most susceptible to flux-induced breakdown.

Consider a film flowing down a vertical heated plate (Fig. 1). We shall call the downstream direction $x$, the direction normal to the plate $z$, and the cross-stream direction $y$. The velocity components in the $(x, y, z)$ directions are called $(u, v, w)$.

First, consider the mean flow down the plate to be given by the laminar-flow balance

$$\mu \frac{\partial^2 u}{\partial z^2} \doteq \rho g. \tag{1}$$

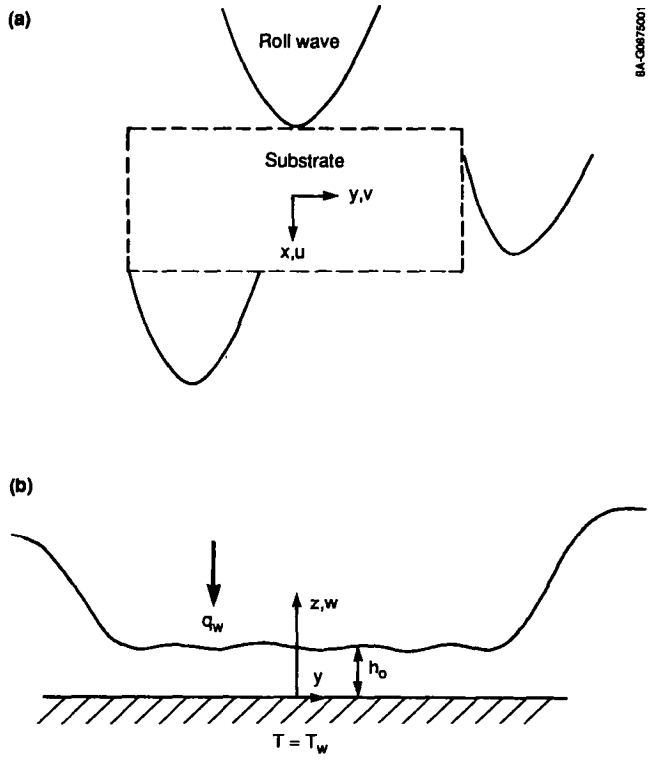


FIG. 1. Nomenclature for the breakdown model.

The Reynolds number of the substrate flow is about two orders of magnitude smaller than that of the main film flow [8]. Therefore, the assumption of laminar film flow in the substrate is reasonable for main film flow Reynolds numbers less than about $10^5$; this covers the range of most industrial applications.

A scale of the 'hydrodynamic' speed $U_H$ is thus given by

$$U_H \doteq \frac{\rho g h_0^2}{\mu} \tag{2}$$

where $h_0$ is an estimate of the mean substrate thickness. Define the Reynolds number of the substrate film flow by

$$Re_s = \frac{U_H h_0}{\nu} \tag{3}$$

so that equations (2) and (3) give

$$h_0 = \left(\frac{\nu^2}{g} Re_s\right)^{1/3}. \tag{4}$$

Second, consider that the interaction of mean flow and thermocapillarity gives rise to structures that resemble rivulets periodic in the cross-stream direction. The thermocapillarity creates surface stresses that drive fluid from troughs into ridges via the cross-stream shear–stress balance at the interface, namely

$$\mu \frac{\partial u}{\partial z} \doteq \frac{d\sigma}{dy} \doteq -\left|\frac{d\sigma}{dT}\right| \frac{\partial T}{\partial y}. \tag{5}$$

An estimate for the 'thermocapillary' speed $U_{TC}$ is thus given by

$$U_{TC} = \left|\frac{d\sigma}{dT}\right| \frac{\Delta T}{\mu} \frac{h_0}{l_y} \tag{6}$$

where $\Delta T$ is an estimate of the temperature differences induced by heating and $l_y$ a lateral length scale. Note that $|d\sigma/dT|$ is a property of the fluid.

Third, the heat balance relates downstream heat convection to conduction normal to the plate

$$\rho c_p u \frac{\partial T}{\partial x} \doteq k \frac{\partial^2 T}{\partial z^2} \sim \frac{\partial q_w}{\partial z}$$

where $q_w$ is the heat flux normal to the plate. If the same estimate, $\Delta T$, for the temperature differences is used, then

$$\Delta T = \frac{l_x}{h_0} \frac{q_w}{\rho c_p U_H} \tag{7}$$

where $l_x$ is a downstream length scale.

Our hypothesis is that a criterion for dryout has the 'thermocapillary' speed large enough compared to the 'hydrodynamic' speed or that

$$\frac{U_{TC}}{U_H} > n\,(\text{constant}). \tag{8}$$

This criterion states that there is a lateral film flow, of magnitude $U_{TC}$, large enough (relative to the downward, gravity-induced film flow) to produce sufficient

thinning of the substrate during its existence between roll waves such that the substrate breaks and forms a stable dry area. Implicit in this development is that the surface is smooth enough so that mean surface tension effects are negligible.

In evaluating equation (8), and in the absence of further information, we make the assumption that $l_x = l_y$ or equivalently that the ratio of the two length scales is constant. The constant $n$ in equation (8) must be evaluated experimentally but should then apply to all falling liquid film systems.

Compare equations (2), (6) and (7) to obtain

$$\frac{U_{TC}}{U_H} = \left|\frac{d\sigma}{dT}\right| \frac{q_W}{\rho c_p \mu} \frac{v^2}{g^2 h_0^4}. \tag{9}$$

Now use equation (4) to obtain the criterion for dryout

$$\frac{q_W}{q_W^{(s)}} > n Re_s^{4/3} \tag{10a}$$

where the scale $q_W^{(s)}$ for the heat flux is given by

$$q_W^{(s)} = \left\{\rho c_p^3 \mu^5 g^2 \left|\frac{d\sigma}{dT}\right|^{-3}\right\}^{1/3}. \tag{10b}$$

Equations (10a) and (10b) state that data for dryout should be expressed as $q_W/q_W^{(s)}$ vs $Re_s$. The derivation hinges on several balances: viscous mean flow driven by gravity downstream, thermocapillary forces driving viscous flow cross-stream, and downstream convection balancing heat conduction normal to the plate.

Property values in equations (10a) and (10b) are to be evaluated at the location of breakdown. If we make the assumption that the substrate Reynolds number is proportional to the overall film Reynolds number, we can replace $Re_s$ on the right-hand side of equation (10a) with $Re$. This will make the resulting correlation easier to use since $Re_s$ is not easily measured.

## 4. EXPERIMENTAL METHODS

As stated above, the constant $n$ in equation (8) must be determined experimentally. The experimental apparatus used to collect the data necessary to determine the constant $n$ is described in detail by Bohn and Carasso [9] and is shown in Fig. 2. Liquid flow was established at the top of a vertical stainless steel tube, 2.54 cm in diameter and 2.5 m long. The tube was polished with 240-grit sandpaper and cleaned with acetone and then ethyl alcohol before testing. Special care was taken to ensure that the tube was straight and plumb. The liquid, either de-ionized water or a mixture of de-ionized water and glycerol (30% glycerol by weight), was uniformly distributed around the top of the tube by an orifice. The temperature of the liquid delivered to the top of the tube was controlled by the heat exchanger shown in Fig. 2. Heat flux was provided by passing a direct current through the tube.

The two test fluids selected have viscosities that differ by about a factor of 3. As shown in the previous section, the breakdown flux is most sensitive to liquid viscosity ($q_W \sim \mu^{5/3}$), so testing with these two liquids provides a reasonably rigorous test of the correlation.

The test procedure first involved establishing a liquid flow rate and inlet temperature. The heat flux was then increased slowly in steps until the initiation of film breakdown was observed near the bottom of the tube. We denoted this heat flux as the breakdown flux, and it was generally repeatable within $\pm 5\%$ for a given set of test conditions.

Electrical power dissipated by the tube was mea-

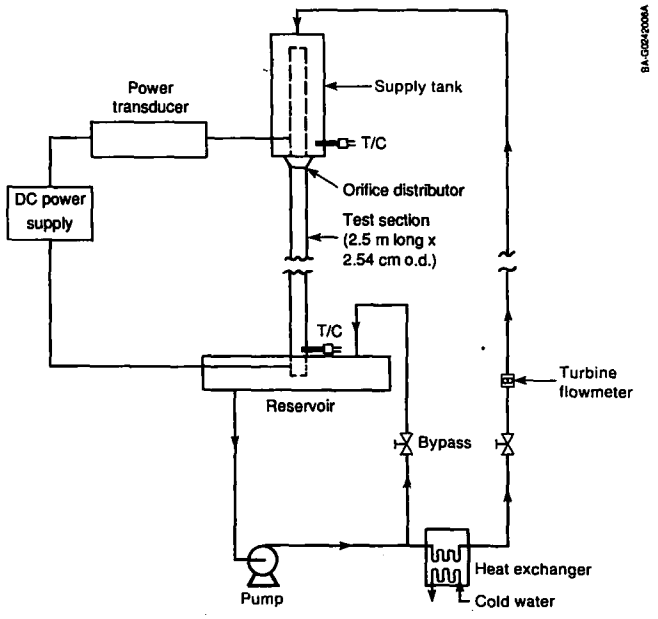


FIG. 2. Vertical-tube falling film apparatus.

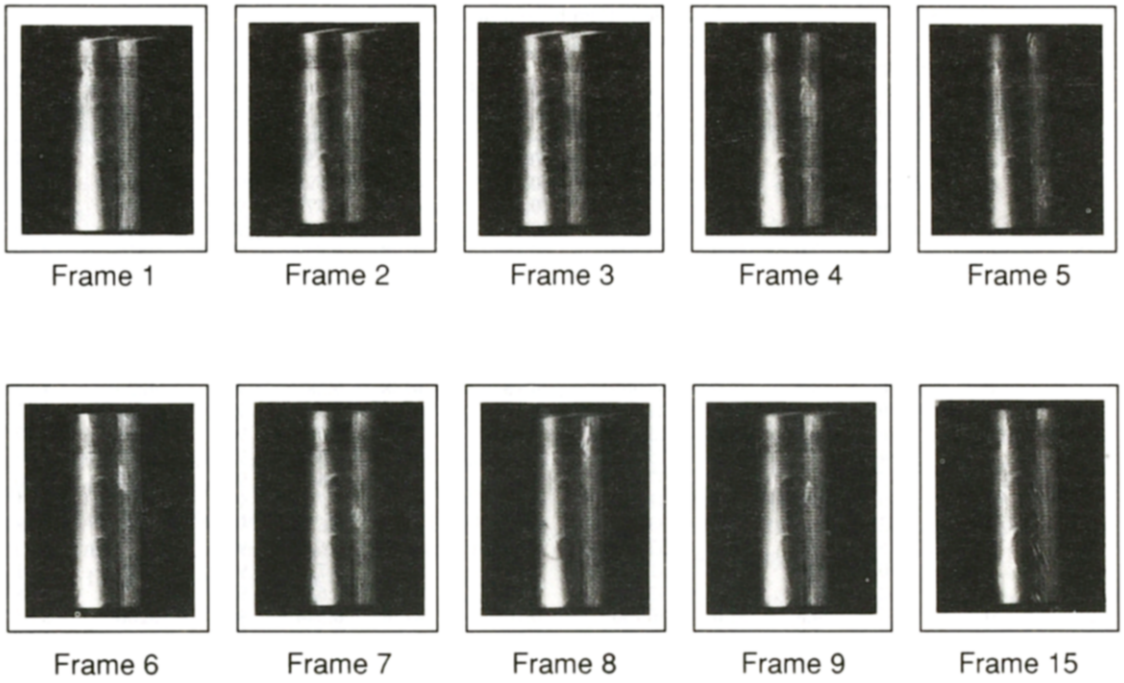


FIG. 3. Sequence of photographs showing the film breakdown process.

sured with a calibrated Hall-effect transducer. Liquid flow rate was measured by a turbine flow meter that had been calibrated by the bucket-and-stopwatch method. Liquid outlet temperature was measured with a type-E thermocouple immersed in the liquid stream at the bottom of the tube.

Data reduction involved nondimensionalizing the breakdown flux to the form prescribed by equations (10a) and (10b), i.e.

$$\frac{q_w}{q_w^{(s)}} = n\,Re^m. \tag{11}$$

As discussed in the previous section, both the nondimensional breakdown flux and the Reynolds number are to be evaluated at local conditions, i.e. at the point of breakdown. Properties of the liquid used were evaluated from published correlations (water: Vargaftik [10]; glycerol–water: Miner and Dalton [11]).

Primary experimental uncertainties include power-transducer calibration-bias and precision errors, liquid-outlet thermocouple-bias and precision errors, and turbine-meter calibration-bias and precision errors. Based on an analysis of these errors, we estimate that the net uncertainty in the reported nondimensional breakdown flux is $\pm 15\%$ and in the breakdown Reynolds number is also $\pm 15\%$.

## 5. FLOW VISUALIZATION

Before describing the experimental results, it is worthwhile to describe the observations made of the breakdown phenomenon. We were able to observe the breakdown process in detail by recording it with a shuttered video camera. The camera provides sequential frames separated by 1/30th of a second with each frame exposed for 1/1000 of a second. A sequence of 10 frames (numbered chronologically 1 through 9 and 15) covering the entire process, about 1/2 s, is shown in Fig. 3. The Reynolds number at the top of the tube was 2500 for this test, and each frame shows a 75 mm vertical extent near the bottom of the tube.

The first observable disturbance in the film was several small pockets of reduced film thickness that can be seen along a vertical line in frame 1 and becoming more distinct in frame 2. In frame 3, these pockets were less pronounced, most likely because a roll wave washed over the pockets, temporarily restoring the film to its undisturbed thickness. The pockets are more distinct in frame 4 and they became more persistant. By frame 6 the pockets formed individual dry spots. The liquid between the small pockets then seemed to thin out. In frame 7 there were two well-defined pockets. By frame 15, one large pocket was formed and that single pocket, i.e. the dry spot, became stable. Diversion of the film flow around the dry spot is clearly visible in the form of small waves on the sides of the dry spot.

## 6. RESULTS AND DISCUSSION

All experimental data are presented in dimensional and nondimensional form in Table 1. The experimental data correlated according to equation (11) are presented in Fig. 4. A least-squares fit to the data give the constants $n = 4.78 \times 10^{-5}$ and $m = 1.43$. The

Table 1. Film breakdown data

| Run No. | Weight % glycerol | Flow rate (gpm) | $T$ inlet (°C) | $T$ outlet (°C) | $q_w$ (W m$^{-2}$) | $\lvert d\sigma/dT\rvert \times 10^3$ (N m$^{-1}$ K$^{-1}$) | $c_p$ (J kg$^{-1}$ K$^{-1}$) | $\mu \times 10^3$ (kg m$^{-1}$ s$^{-1}$) | $\rho$ (kg m$^{-3}$) | $Re$ @ breakdown (—) | $q_w/q_w^{(s)}$ (—) |
|---|---|---|---|---|---|---|---|---|---|---|---|
| 1 | 0 | 2.00 | 8.8 | 34.5 | 90 000 | 0.167 | 4178 | 0.758 | 991 | 8363 | 12.48 |
| 2 | 0 | 1.00 | 7.2 | 46.8 | 55 500 | 0.167 | 4178 | 0.598 | 986 | 5299 | 11.42 |
| 3 | 0 | 1.00 | 7.9 | 33.6 | 40 500 | 0.167 | 4178 | 0.771 | 992 | 4108 | 5.45 |
| 4 | 0 | 1.00 | 6.2 | 39.4 | 44 200 | 0.167 | 4178 | 0.688 | 989 | 4609 | 7.20 |
| 5 | 0 | 1.00 | 7.0 | 29.9 | 33 700 | 0.167 | 4178 | 0.832 | 993 | 3812 | 4.00 |
| 6 | 0 | 1.00 | 7.9 | 43.5 | 45 000 | 0.167 | 4178 | 0.636 | 988 | 4981 | 8.36 |
| 7 | 0 | 1.00 | 3.9 | 41.4 | 51 000 | 0.167 | 4178 | 0.662 | 989 | 4794 | 8.86 |
| 8 | 0 | 1.00 | 11.4 | 41.0 | 40 500 | 0.167 | 4178 | 0.667 | 989 | 4743 | 6.95 |
| 9 | 0 | 1.00 | 14.7 | 44.3 | 41 200 | 0.167 | 4178 | 0.627 | 987 | 5043 | 7.85 |
| 10 | 0 | 1.00 | 7.6 | 44.4 | 65 200 | 0.167 | 4178 | 0.625 | 987 | 5067 | 12.45 |
| 11 | 0 | 1.00 | 8.3 | 39.6 | 48 000 | 0.167 | 4178 | 0.685 | 989 | 4623 | 7.87 |
| 12 | 0 | 0.50 | 5.2 | 33.7 | 21 000 | 0.167 | 4178 | 0.770 | 992 | 2060 | 2.83 |
| 13 | 0 | 0.26 | 6.1 | 46.2 | 15 700 | 0.167 | 4178 | 0.605 | 987 | 1363 | 3.17 |
| 14 | 0 | 0.34 | 7.1 | 40.5 | 15 000 | 0.167 | 4178 | 0.674 | 989 | 1600 | 2.53 |
| 15 | 0 | 0.75 | 8.1 | 42.6 | 37 100 | 0.167 | 4178 | 0.647 | 988 | 3672 | 6.70 |
| 16 | 0 | 0.90 | 5.0 | 37.5 | 41 200 | 0.167 | 4178 | 0.714 | 990 | 3999 | 6.31 |
| 17 | 0 | 0.62 | 5.6 | 42.2 | 33 000 | 0.167 | 4178 | 0.652 | 988 | 3016 | 5.88 |
| 18 | 0 | 0.75 | 8.1 | 42.6 | 37 100 | 0.167 | 4178 | 0.647 | 988 | 3672 | 6.70 |
| 19 | 0 | 0.90 | 5.0 | 37.5 | 41 200 | 0.167 | 4178 | 0.714 | 990 | 3999 | 6.31 |
| 20 | 0 | 0.62 | 5.6 | 42.2 | 33 000 | 0.167 | 4178 | 0.652 | 988 | 3016 | 5.88 |
| 21 | 0 | 0.55 | 4.8 | 52.0 | 36 700 | 0.167 | 4178 | 0.544 | 984 | 3206 | 8.85 |
| 22 | 0 | 0.30 | 5.6 | 39.8 | 15 800 | 0.167 | 4178 | 0.683 | 989 | 1394 | 2.61 |
| 23 | 0 | 0.31 | 5.4 | 34.4 | 15 000 | 0.167 | 4178 | 0.759 | 991 | 1295 | 2.07 |
| 24 | 0 | 0.39 | 4.8 | 33.6 | 17 200 | 0.167 | 4178 | 0.771 | 992 | 1604 | 2.31 |
| 25 | 0 | 0.50 | 4.6 | 28.4 | 19 100 | 0.167 | 4178 | 0.858 | 994 | 1849 | 2.15 |
| 26 | 0 | 0.61 | 3.2 | 28.6 | 22 500 | 0.167 | 4178 | 0.854 | 994 | 2267 | 2.55 |
| 27 | 0 | 0.72 | 4.7 | 28.9 | 25 500 | 0.167 | 4178 | 0.849 | 994 | 2691 | 2.92 |
| 28 | 0 | 0.80 | 4.6 | 29.5 | 28 500 | 0.167 | 4178 | 0.838 | 993 | 3027 | 3.33 |
| 29 | 0 | 0.91 | 4.6 | 37.5 | 38 200 | 0.167 | 4178 | 0.714 | 990 | 4044 | 5.85 |
| 30 | 0 | 1.00 | 6.3 | 41.0 | 43 800 | 0.167 | 4178 | 0.667 | 989 | 4753 | 7.51 |
| 31 | 0 | 1.11 | 5.6 | 47.8 | 47 800 | 0.167 | 4178 | 0.587 | 986 | 5995 | 10.15 |
| 32 | 0 | 1.23 | 4.5 | 36.9 | 44 200 | 0.167 | 4178 | 0.722 | 990 | 5403 | 6.64 |
| 33 | 0 | 1.12 | 4.4 | 48.1 | 51 000 | 0.167 | 4178 | 0.584 | 986 | 6085 | 10.93 |
| 34 | 0 | 1.10 | 5.2 | 40.1 | 45 700 | 0.167 | 4178 | 0.679 | 989 | 5141 | 7.61 |
| 35 | 0 | 1.10 | 6.1 | 38.0 | 48 700 | 0.167 | 4178 | 0.707 | 990 | 4934 | 7.58 |
| 36 | 0 | 0.80 | 4.1 | 50.5 | 44 200 | 0.167 | 4178 | 0.559 | 985 | 4541 | 10.19 |
| 37 | 0 | 0.82 | 4.3 | 48.8 | 45 000 | 0.167 | 4178 | 0.577 | 986 | 4513 | 9.85 |
| 38 | 0 | 0.92 | 4.2 | 50.6 | 50 200 | 0.167 | 4178 | 0.558 | 985 | 5231 | 11.61 |
| 39 | 0 | 0.90 | 10.4 | 53.6 | 44 600 | 0.167 | 4178 | 0.529 | 984 | 5386 | 11.28 |
| 40 | 0 | 0.92 | 13.7 | 51.4 | 42 700 | 0.167 | 4178 | 0.550 | 985 | 5287 | 10.11 |
| 41 | 0 | 0.91 | 17.1 | 59.4 | 45 700 | 0.167 | 4178 | 0.478 | 981 | 6008 | 13.68 |
| 42 | 0 | 0.91 | 18.3 | 58.9 | 45 000 | 0.167 | 4178 | 0.482 | 982 | 5954 | 13.28 |
| 43 | 0 | 0.91 | 19.5 | 57.1 | 45 000 | 0.167 | 4178 | 0.497 | 982 | 5769 | 12.61 |
| 44 | 0 | 0.60 | 5.9 | 48.0 | 37 500 | 0.167 | 4178 | 0.585 | 986 | 3252 | 8.01 |
| 45 | 0 | 0.56 | 5.6 | 50.1 | 35 200 | 0.167 | 4178 | 0.563 | 985 | 3154 | 8.02 |
| 46 | 0 | 0.50 | 6.0 | 44.7 | 26 200 | 0.167 | 4178 | 0.622 | 987 | 2549 | 5.05 |
| 47 | 0 | 0.49 | 6.0 | 37.0 | 20 200 | 0.167 | 4178 | 0.721 | 990 | 2155 | 3.04 |
| 48 | 0 | 0.55 | 5.8 | 33.5 | 19 900 | 0.167 | 4178 | 0.773 | 992 | 2257 | 2.67 |
| 49 | 0 | 0.61 | 5.9 | 36.9 | 24 400 | 0.167 | 4178 | 0.722 | 990 | 2678 | 3.66 |
| 50 | 0 | 0.65 | 6.8 | 37.2 | 24 000 | 0.167 | 4178 | 0.718 | 990 | 2869 | 3.64 |
| 51 | 0 | 0.71 | 6.3 | 38.5 | 28 500 | 0.167 | 4178 | 0.700 | 990 | 3216 | 4.51 |
| 52 | 0 | 0.75 | 6.3 | 38.8 | 31 900 | 0.167 | 4178 | 0.696 | 990 | 3417 | 5.10 |
| 53 | 0 | 1.00 | 7.3 | 61.6 | 68 200 | 0.167 | 4178 | 0.461 | 981 | 6880 | 21.74 |
| 54 | 0 | 0.80 | 7.6 | 68.5 | 65 200 | 0.167 | 4178 | 0.411 | 978 | 6168 | 25.16 |
| 55 | 0 | 0.82 | 7.0 | 61.2 | 60 700 | 0.167 | 4178 | 0.464 | 981 | 5604 | 19.13 |
| 56 | 0 | 0.69 | 7.9 | 50.2 | 43 500 | 0.167 | 4178 | 0.562 | 985 | 3889 | 9.94 |
| 57 | 0 | 0.61 | 7.4 | 48.3 | 36 400 | 0.167 | 4178 | 0.582 | 986 | 3322 | 7.85 |
| 58 | 0 | 0.51 | 7.5 | 47.3 | 27 700 | 0.167 | 4178 | 0.593 | 986 | 2727 | 5.79 |
| 59 | 30 | 0.57 | 4.6 | 39.7 | 27 700 | 0.136 | 3635 | 1.371 | 1066 | 1417 | 1.31 |
| 60 | 30 | 0.80 | 4.4 | 43.6 | 44 200 | 0.136 | 3635 | 1.225 | 1064 | 2227 | 2.53 |
| 61 | 30 | 0.50 | 3.8 | 31.1 | 18 700 | 0.136 | 3635 | 1.777 | 1069 | 959 | 0.57 |
| 62 | 30 | 0.61 | 3.7 | 47.5 | 34 500 | 0.136 | 3635 | 1.097 | 1063 | 1897 | 2.37 |
| 63 | 30 | 0.72 | 4.0 | 50.3 | 42 000 | 0.136 | 3635 | 1.015 | 1062 | 2419 | 3.29 |
| 64 | 30 | 0.81 | 5.5 | 46.6 | 44 200 | 0.136 | 3635 | 1.125 | 1063 | 2454 | 2.91 |
| 65 | 30 | 0.51 | 8.7 | 48.5 | 30 000 | 0.136 | 3635 | 1.067 | 1062 | 1628 | 2.16 |
| 66 | 30 | 0.51 | 5.3 | 37.1 | 22 500 | 0.136 | 3635 | 1.481 | 1066 | 1174 | 0.94 |
| 67 | 30 | 0.51 | 7.1 | 43.1 | 28 500 | 0.136 | 3635 | 1.242 | 1064 | 1398 | 1.59 |
| 68 | 30 | 0.52 | 12.3 | 35.5 | 18 700 | 0.136 | 3635 | 1.553 | 1067 | 1138 | 0.72 |
| 69 | 30 | 0.53 | 15.0 | 38.9 | 20 200 | 0.136 | 3635 | 1.404 | 1066 | 1283 | 0.92 |
| 70 | 30 | 0.52 | 18.2 | 44.1 | 22 500 | 0.136 | 3635 | 1.207 | 1064 | 1462 | 1.32 |

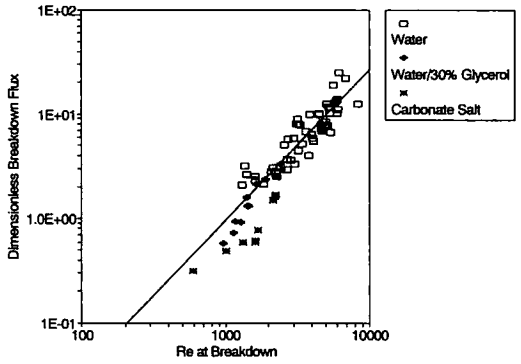


FIG. 4. Correlation of experimental data, scaled heat flux vs film Reynolds number.

r.m.s. error between the correlation for dimensionless breakdown flux and the experimental data is 2.6. Note that the model as described by equation (10a) gives an exponent of 4/3 compared to the experimental value of 1.43. The correlation is then

$$\frac{q_w}{q_w^{(s)}} = 4.78 \times 10^{-5} Re^{1.43}. \quad (12)$$

Since the correlation collapses the data reasonably well, our assumption that the substrate Reynolds number is proportional to the overall film Reynolds number is justified.

In addition to the data for water and the water–glycerol test fluids, Fig. 4 presents data taken on a second experimental apparatus with a molten salt. This apparatus and a discussion of experimental uncertainties has been described in detail by Bohn *et al.* [12]. Briefly, a film of molten salt (the eutectic of lithium, sodium, potassium carbonate with a viscosity about six times that of water) was distributed across the top of a 152 mm wide by 610 mm long flat plate tilted back 5° from vertical. A weir distributor was used to introduce the salt at the top of the plate. Heat flux was provided by concentrated solar energy supplied by a central receiver facility. By reducing salt flow at constant heat flux, it was possible to cause the film to break, as was observed by the presence of a dry patch in the film and excessive plate temperatures. In addition to plate temperatures, salt flow rate, heat flux, and salt temperatures were measured. The measured heat flux was nondimensionalized according to equation (11) above and plotted with the water and water–glycerol data in Fig. 4.

These molten salt data should be considered to be qualitative because they were taken before development of the correlation and with the intent of only providing an initial bound on the breakdown flux as a function of molten salt flow rate. Nevertheless, it is worthwhile to include these data in the comparison with the correlation. Considering the qualitative nature of the data, the comparison with the correlation line is reasonably good. We note that these data fall below the correlation line and that this could be due to two features of the experiment. First, the total film flow length was only 1 m and the wavy film was not fully developed. This may affect some of the assumptions in the correlation. In addition, the film was tilted 5° back from vertical adding a hydrostatic force to the film. This would tend to slightly stabilize the film against thermocapillary disturbances.

## 7. CONCLUSIONS

A heated falling film in the roll-wave regime is susceptible to breakdown and rivulet formation. By focusing on local force balances in the substrate we have obtained a new correlation for breakdown heat flux vs film Reynolds number. Flow visualization has elucidated the breakdown process and film flow experiments have given data on breakdown at higher heat fluxes and Reynolds numbers than were available in the past. The correlation gives one the ability to predict the thermocapillary breakdown of wavy falling-films at high Reynolds number, high heat flux, and over a wide range of fluid properties.

*Acknowledgements*—Prepared for the U.S. Department of Energy, Contract No. DE-AC02-83CH10093. James Siebarth is gratefully acknowledged for his assistance in collecting the experimental data.

## REFERENCES

1. T. A. Newell, K. Y. Wang and R. J. Copeland, Falling film flow characteristics of the direct absorption receiver, SERI/TR-252-2641., Solar Energy Research Institute, Golden, Colorado (1986).
2. J. C. Chung and S. G. Bankoff, Initial breakdown of a heated liquid film in cocurrent two-component annular flow: II. Rivulet and drypatch models, *Chem. Engng Commun.* **4**, 455–470 (1980).
3. S. W. Joo, S. H. Davis and S. G. Bankoff, A mechanism for rivulet formation in heated falling films, Appl. Math. Tech. Report #9110, Northwestern University, and pending publication (1993).
4. K. J. Chu and A. E. Dukler, Statistical characteristics of thin, wavy films, III. Structure of the large waves and their resistance to gas flow, *A. I. Ch. E. Jl* **21**, 583–593 (1975).
5. W. S. Norman and V. McIntyre, Heat transfer to a liquid film on a vertical surface, *Trans. Inst. Chem. Engrs* **38**, 301–307 (1960).
6. F. S. Simon and Y.-Y. Hsu, Thermocapillary induced breakdown of a falling liquid film, NASA TN D-5624, National Aeronautics and Space Administration, Washington, DC (1970).
7. T. Fujita and T. Ueda, Heat transfer to falling liquid films and film breakdown, *Int. J. Heat Mass Transfer* **21**, 97–108 (1978).
8. A. E. Dukler, The role of waves in two phase flow: some new understanding, 1976 Award Lecture, *Chem. Engng Educ.* 108–138 (1977).
9. M. S. Bohn and M. Carasso, Direct absorption receiver final technical report, SERI/TR-253-3438, Solar Energy Research Institute, Golden, Colorado (1989).
10. N. B. Vargaftik, *Handbook of Physical Properties of Liquids and Gases*, 2nd edn. Hemisphere, Washington, DC (1975).
11. C. S. Miner and N. N. Dalton (Eds), *Glycerol.* Reinhold, New York (1953).
12. M. S. Bohn, H. J. Green, G. P. Yeagle, J. E. Siebarth, O. D. Asbell and C. T. Brown, Direct absorption receiver experiments and concept feasibility, SERI/TR-252-2684, Solar Energy Research Institute, Golden, Colorado (1988).